Type of the Paper (Article, Review, Communication, etc.)

A Green Procedure to Manufacture Nanoparticle Decorated Paper Substrates

Werner Schlemmer [1], Wolfgang Fischer [1], Armin Zankel [2], Tomislava Vukušić [3], Gregor Filipič [4], Andrea Jurov [4,5], Damjan Blažeka [6], Walter Goessler[7], Wolfgang Bauer[1], Stefan Spirk [1,*] and Nikša Krstulović [6,*]

[1] Graz University of Technology, Institute of Paper-, Pulp- and Fibre Technology (IPZ), Inffeldgasse 23, 8010 Graz, Austria.
[2] Institute of Electron Microscopy and Nanoanalysis (FELMI), Steyrergasse 17, 8010 Graz, Austria.
[3] Faculty of Food Technology and Biotechnology, University of Zagreb, Pierottijeva 6, 10000 Zagreb, Croatia
[4] Jožef Stefan Institute, Jamova 39, Ljubljana 1000, Slovenia
[5] Jožef Stefan International Postgraduate School, Jamova 39, Ljubljana 1000, Slovenia
[6] Institute of Physics, Bijenička 46, 10000 Zagreb, Croatia
[7] Institute of Chemistry, University of Graz, Universitaetsplatz 1, 8010 Graz, Austria
* Correspondence: niksak@ifs.hr ; Tel.: +385-1-4698-803
stefan.spirk@tugraz.at; Tel.: +43-316-873-30763

Abstract: A paper impregnated with silver nanoparticles (AgNPs) has been prepared. For the preparation of the substrates, aqueous suspensions of pulp fines, a side product from the paper production, have been mixed with Ag nanoparticles (AgNP) suspensions. The nanoparticle synthesis thereof was carried out via laser ablation of pure Ag in water. After the sheet formation process, the leaching of the AgNPs was determined to be low while the sheets exhibited antimicrobial activity towards *E. Coli*.

Keywords: silver nanoparticles; laser ablation in liquids; laser synthesis of colloidal nanoparticle solution, nanoparticle impregnated paper; antimicrobial activity; fiber fines; sheet forming; vacuum filtration

1. Introduction

Cellulose, a biopolymer consisting β-D 1→4 linked glucose, is the main component in many industrial products such as pulp and paper. In recent years, the development of micro and nanostructured materials (e.g., nano and microfibrillated cellulose) was a boost to cellulose science and new applications for industrial purposes have been proposed. One way to create such new materials is to include inorganic matter having particular properties. In this context, the incorporation of functional inorganic nanoparticles (e.g., antimicrobial, conductive, photoactive, catalysts, magnetic) into different types of cellulosic substrates has been described for many cellulosic materials [1-8]. In principle, there are different ways how nanoparticles can be implemented into these materials. One approach is the so called in-situ synthesis, where the nanoparticle precursor, typically a metal salt, is added to a cellulosic material. The metal ions are coordinating to the cellulose macromolecules and a chemical reaction is induced to convert the salt into either metal, metal oxide or metal sulfide nanoparticles, which are formed in close spatial proximity to the cellulose material [9]. In this way, silver and gold nanoparticle decorated fibers have been prepared from $AgNO_3$ and $HAuCl_4$, in the presence of different types of reduction agents [10-11]. While $NaBH_4$ was frequently used in older studies to reduce the metal salts, in recent years the use of environmentally friendly reduction agents became more popular. Here, either glucose, or polysaccharides with reducing end groups (i.e. aldehydes) were used to generate silver and gold nanoparticles [12-16]. Particularly, polysaccharides are interesting since they do not only act as reduction agent but also serve as electrosteric stabilizers preventing aggregation of the nanoparticles providing suspensions which can be stable for several months [17].

A different route comprises the application of the ready-made nanoparticles to a cellulosic material, and then to perform a processing step. If the nanoparticles are stabilized by a polymer shell, covalent or physical binding onto the cellulosic substrate can be additionally performed. For instance, silver and gold nanoparticles have been synthesized and encapsulated by sulfated chitosans showing antithrombogenic behavior [3,18]. After immobilization on surfaces, simultaneous antimicrobial and anticoagulant surfaces were obtained.

These methods have in common that a metal salt precursor is required which needs to be converted to the desired nanoparticles, very often using elevated temperatures that give a particular type of nanoparticle shape (e.g., spheres, rods). In most cases, nanoparticles contain either capping agents or polymer shells to prevent agglomeration and to obtain stable colloidal suspensions. However, the largest drawback of many wet-chemical routes is their yield which is hardly ever reported in scientific papers (even in our own papers on the topic). In order to overcome limitations and to make the production of nanoparticles more scalable and environmentally friendly, laser ablation in liquids (LAL) has been proposed recently for nanoparticle preparation [19]. This technique is based on the process of pulsed laser ablation of a target (metals, metal oxides, nitrides etc.) immersed in a liquid [20,21,22]. There are many advantages of this technique over standard ones but its potential is still not fully exploited to full extent so far. It is known as a 'green synthesis' technique since additional chemicals are not required [23] while the formation of any residues or by-products is prevented. In principle pure nanoparticles can be obtained that do not contain any residues on the surface, except oxidation products (e.g., silver oxides). The LAL technique is not limited by the choice of materials as any metal target or target made of other materials (composites, isolators, conductive materials, semiconductors, organic materials, ceramics, catalytic, hybrid and magnetic or paramagnetic materials) can be used for the synthesis of colloidal nanoparticle suspensions. The synthesis can be carried out in a wide variety of liquids for tailoring the nanoparticles properties [24,25]. Laser pulses can additionally generate, de-agglomerate, fragmentate, re-shape and reduce the size of the initially formed nanoparticles either by secondary laser interaction (post-irradiation) [26-29] or by double-pulse LAL [30-32].

In this paper, we explore how to use LAL for the preparation of AgNPs nanoparticles (AgNPs) in water and to integrate these in a paper based substrate, consisting of fine cellulosic microparticles. Sheets from such fine cellulosic particles resemble to a significant extent to those made of microfibrillated cellulose, a recently proposed material for many applications such as barrier coatings and packaging materials but the price of the material is much lower since it is a large scale underutilized material in cellulose processing industries. The outline of the paper is as follows: after description of the synthesis/characterization of the NPs by laser ablation, the procedure to incorporate nanoparticles into sheets made from fines is described. At the end of the paper, the properties of the substrates in terms of antimicrobial activity as well as the leaching of AgNPs from the material is evaluated.

2. Materials and Methods

Laser synthesis of nanoparticles

A colloidal solution of AgNPs was synthesized using pulsed laser ablation of a Ag plate (purity 99.99%, thickness 1 mm, Kurt J. Lesker) immersed in a cuvette filled with 25 mL of deionized water. Laser ablation was conducted with a Nd:YAG laser (Quantell, Brilliant) using the following specifications: pulse duration 5 ns, wavelength 1064 nm, output energy 290 mJ, repetition rate 5 Hz. The target was fixed on the holder in order to drill craters during ablation. The laser beam was focused by a 10 cm lens onto the target surface. The laser pulse energy in front of the target was 120 mJ while a diameter of a focused pulse on the target surface was 1 mm yielding a laser fluence of 15 J/cm^2. The thickness of a water layer above the target was kept constant at 1.5 cm during the experiment in order to keep the ablation efficiency constant [33]. A detailed scheme of experimental setup for laser ablation in water is shown in [34].

The morphology of AgNPs was observed using a transmission electron microscope (TEM, FEI Tecnai G2 20 Twin). Obtained TEM pictures were used to calculate size-distribution of the AgNPs.

Peer-reviewed version available at Materials 2018, 11, 2412; doi:10.3390/ma11122412

After the ablation, the crater created on the Ag target was studied by an optical microscope (Leitz, Leica Aristomet, reflective illumination mode) in order to determine the crater's volume for the assessment of nanoparticle concentration in a procedure described in [35]. The procedure on how the crater volume is determined is described in detail in [36]. The concentration of AgNPs is determined to be of order of 10^{10} mL^{-1}.

A colloidal solution of laser-synthesized AgNPs was analyzed using a spectrophotometer (Perkin Elmer, Lambda 25) to assess the UV-Vis absorption spectrum. Zeta potential ζ (Malvern Zetasizer) of Ag colloidal solution is measured to be -50 mV what indicating a colloidal solution of high stability (the solution is stable for months).

AgNP impregnated fines sheets were analyzed by SEM (Jeol JSM-7600F). The electron accelerating voltage was set to 10 kV. Before the imaging, samples were coated with a thin layer of amorphous carbon (PECS 682) to prevent charge accumulation on the surface. Observation mode was set to low-energy secondary electron detection. EDS was done on the same instrument by INCA Oxford 350 EDS SDD detector and an accelerated potential of 15 kV.

Hand sheet formation

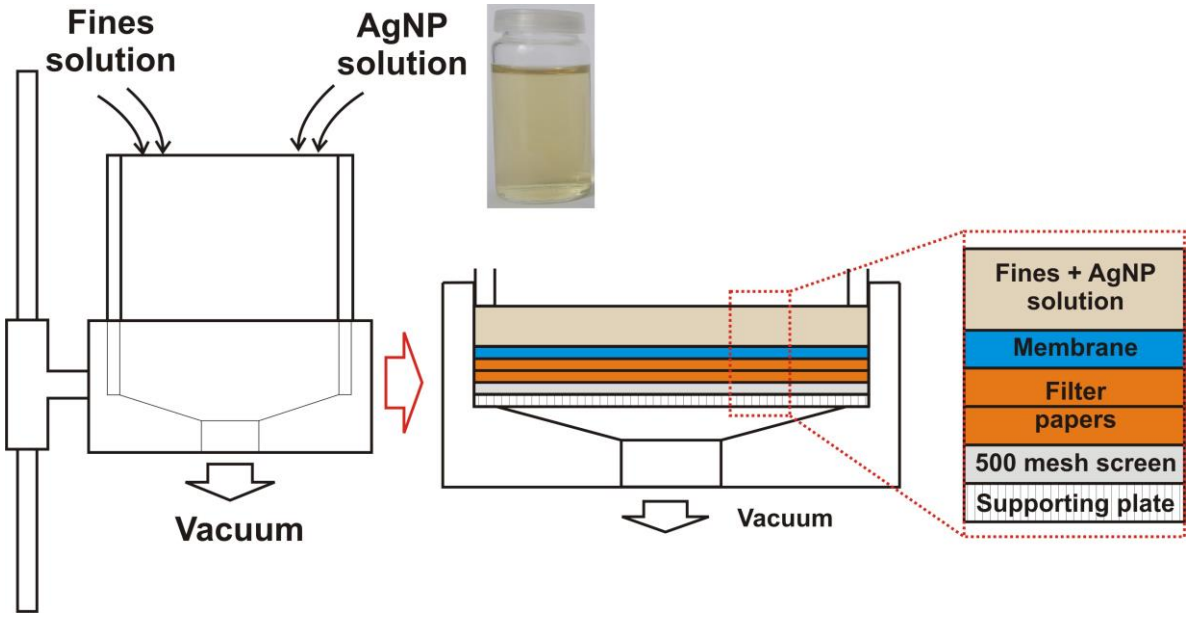

Figure 1. Scheme of the manufacturing process of preparing AgNP impregnated sheets.

All tests have been performed using primary fines separated from never-dried, bleached sulfite pulp (mixture of spruce and beech). In order to prepare hand sheets from pure fines, a vacuum filtration method described in [37] is used. A defined amount of fines (0.24 g, dry weight) is diluted with deionized water to reach a solid content of 0.24 wt %. This suspension is stirred at 450 rpm for at least 2 h. After stirring, 2 mL of AgNP colloidal solution (10^{10} particles mL^{-1}) is added in the suspension and stirred for 5 minutes. After addition of AgNPs, the sheets are formed by vacuum filtration using a Britt Dynamic Drainage Jar (Frank PTI, Birkenau, Germany). The scheme used for AgNP impregnated sheet forming is shown in Figure 1.

The Britt Dynamic Drainage Jar is equipped with a supporting plate, a 500-mesh screen (hole diameter 20 m), two filter papers, and a nitrocellulose membrane (DAWP29325 from Merck Chemicals and Life Science GesmbH, Darmstadt, Germany) with a pore size of 0.65 µm. The major advantage of using the Britt Dynamic Drainage Jar as compared to a Büchner funnel is to improve the fines sheet formation. In particular, the sandwich-like setup prevents the loss of fine cellulosic material. After the filtration step, the membrane with the fines/MFC sheet on top is pre-dried in a Rapid-Köthen sheet dryer (Frank PTI, Birkenau, Germany) for about 20 s at 93 °C under vacuum. Then, the membrane is peeled off, and the neat fines/MFC sheets are dried for 10 min in the Rapid-

Köthen sheet dryer. The sheets are then stored in a climate room at 23 °C and 50% RH for least 12 h prior to testing.

From known concentration of AgNPs, volume of colloidal AgNPs added to the suspension and sheet dimension (10 cm in diameter), the density of impregnated AgNPs can be calculated. It yields that the number density of impregnated AgNPs is in the order of 10 nanoparticles per μm^2.

Antimicrobial test

For the determination of antimicrobial activity *E. coli* K12 was used. The bacterial suspension was prepared by inoculating 20 µL of *E. coli* K12 in 10 ml of Nutrient broth (Biolife, Milan, Italy). This bacterial suspension was incubated at 37 °C for 24 h to create bacteria in the stationary growth phase. Incubated bacterial suspension was centrifuged (Tehtnica, Centric 150) at 4000 rpm for 10 min at room temperature. Harvested cells were washed three times and re-suspended in phosphate buffer saline (PBS) and sterile water solution.

Paper impregnated with AgNPs was inoculated using 10-100 µL of the selected microorganism and placed in an Eppendorf tube containing phosphate buffer. The aliquot sample was incubated 0h, 1h, 4h, 6h and 24h, respectively, after the addition of *E. coli* K12 at a temperature of 37 °C. After incubation, the number of microorganisms (CFU/mL) was determined by the standard dilution method on Nutrient agar (Biolife, Milan, Italy). As a control, the selected microorganism (100 µL) was inoculated into 900 µL of phosphate buffer, incubated and counted by the number of augmented cells. The results were reported as log colony forming units per milliliter (log CFU/mL).

Leaching tests and analysis of the solutions

To investigate the leaching of AgNPs upon contact with water the paper substrates were shaken in ultrapure water and samples of the liquid were taken after 5 min, 10 min, 30 min, 1 h, 2 h, 5 h, 8h and 24h. The total Ag concentration in these extracts was determined after acidification with nitric acid (10 % v/v) with an Agilent 7700cx ICPMS at m/z 107. The NIST CRM 1640a *Trace elements in water* was used for quality control.

3. Results

AgNPs feature surface plasmons (SP) activated by interaction of conductive electrons and an external electromagnetic field, *i.e.* via irradiation with light. If these photons have the right frequency (*i.e.* the plasmonic frequency), the SPs are excited into a resonant state, oscillating with the highest possible amplitude. This plasmonic frequency depends on the size, shape, chemical composition and environment of the NPs. From the frequency (wavelength) dependency on the intensity (i.e. absorbance) of the colloidal NPs, which can be assessed by UV-Vis spectroscopy, one can roughly estimate the NPs size in solution. For more information on SPR, we refer to the very instructive review article by Schlücker et al. [10].

In Figure 2 (a), a UV-Vis spectrum and (b) the size-distribution of the LAL synthesized AgNPs is shown. The UV-Vis spectrum of the AgNPs synthesized by laser ablation shows a distinct maximum at 400 nm typical for surface plasmon resonance of Ag nanoparticles with dimension of few tens of nanometers [10]. This rough estimation is further supported by TEM analysis (inset of Figure 2 (b)), which, in addition, reveals that the AgNPs have a spherical shape. The AgNP feature an average dimension of 28 nm and their size distribution is relatively broad (FWHM of 20 nm; fitting by a Log-Normal function (black line)). The LogN fit is often used to describe the size-distribution of the nanoparticles synthesized from the gaseous phase which is the case in nanoparticles syntheses processes by LAL. It applies whenever particle growth depends on diffusion and drift of atoms to a growth zone of nanoparticles [39]. The final distribution is determined by the available growth time of the nanoparticles [40]. The formation of AgNPs synthesized by LAL is described by dynamic formation mechanisms which includes a diffusion slow-growth (diffusion coalescence) process [41-43].

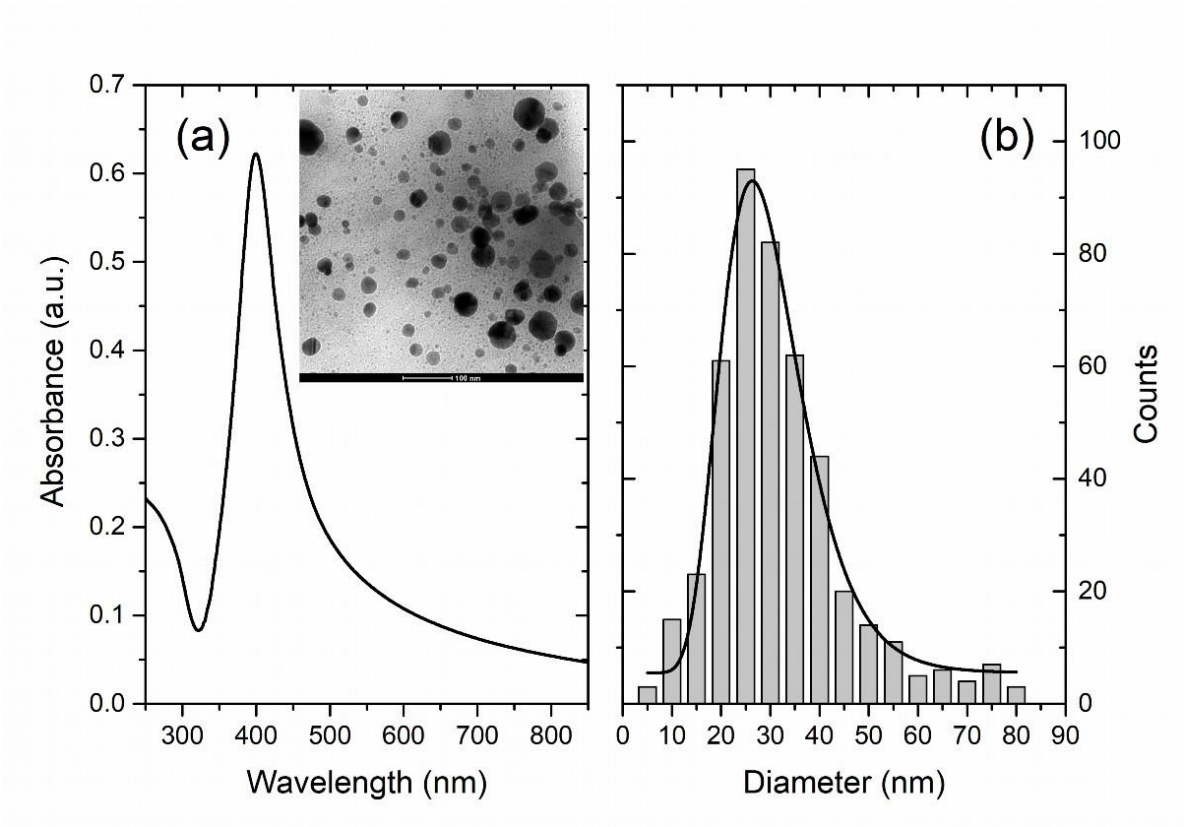

Figure 2: (a) UV-Vis photoabsorptuion spectra of colloidal AgNP (Inset: TEM image of AgNPs) and (b) Size-distribution of AgNPs obtained by TEM imaging (black line – LogNormal fit)

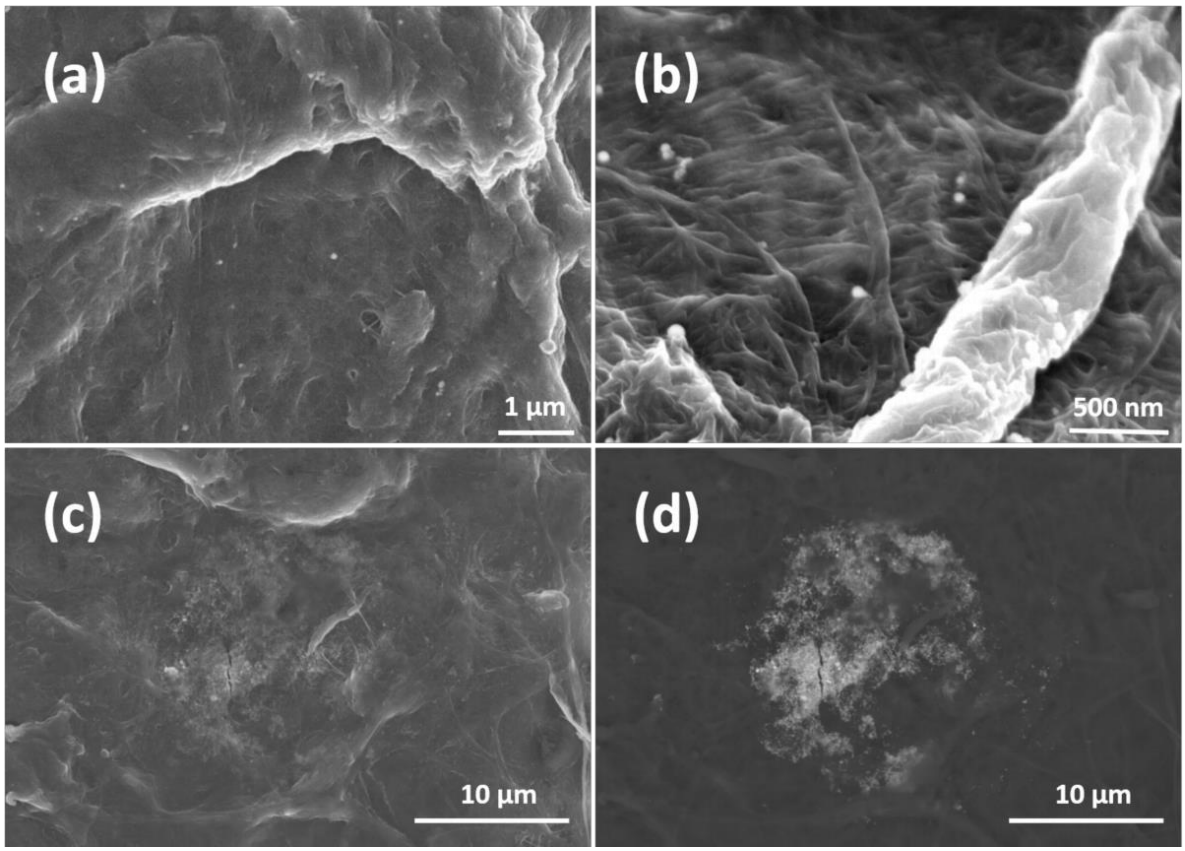

Figure 3. SEM images of AgNP impregnated sheets at different magnifications (a) and (b). (c) and (d) are the same image recorded with different detectors to show impregnated agglomerates.

After characterization, these nanoparticles were implemented into a sheet forming process. Suspensions containing the AgNPs and the paper fines were mixed and a stable colloidal suspension was obtained. This suspension was then applied to a Britt Jar process in order to avoid any loss of fine cellulosic material as described in [37]. Afterwards, the sheets were transferred to a drying system and hand sheets were obtained.

Figure 3 depicts SEM images of such AgNP impregnated hand sheets at different magnification. In Figure 3 (a) and (b), distinct AgNPs located at the surface of the sheets can be observed. Identification of the AgNPs was further performed by EDS measurements (not shown here). Figure 3 (c) and (d) depict the same images but recorded with different detectors. They reveal AgNP agglomerates (which are very rare) embedded beneath the sheet surface, covered with much smaller fines fibers. AgNPs in (a) and (b) are in direct while those in (c) and (d) are in close contact with bacteria in antimicrobial testing experiments since the sheets are hydrophilic. In Figure 3 (a) and (b) one can identify only few AgNP per μm^2 on the sheet surface. It implies that AgNPs are impregnated in the whole volume of the sheet as their density is around 10 AgNP per μm^2. It can be clearly seen that the AgNP are hardly agglomerated, which relates to the processing conditions. There, the AgNPs colloidal suspensions are added to the fines suspensions under rigorous stirring which ensure an even distribution of the AgNP in the fines suspension and consequently in the formed sheets.

These papers have been subjected to antibacterial tests using *E. Coli* K12. As indicated in Figure 4, the impregnated materials are highly active towards *E. Coli* K12. Figure 4 shows antimicrobial activity of AgNP during 24h, where it can be seen that AgNP antibacterial activity is increasing in time reaching up to 4 log reduction rate.

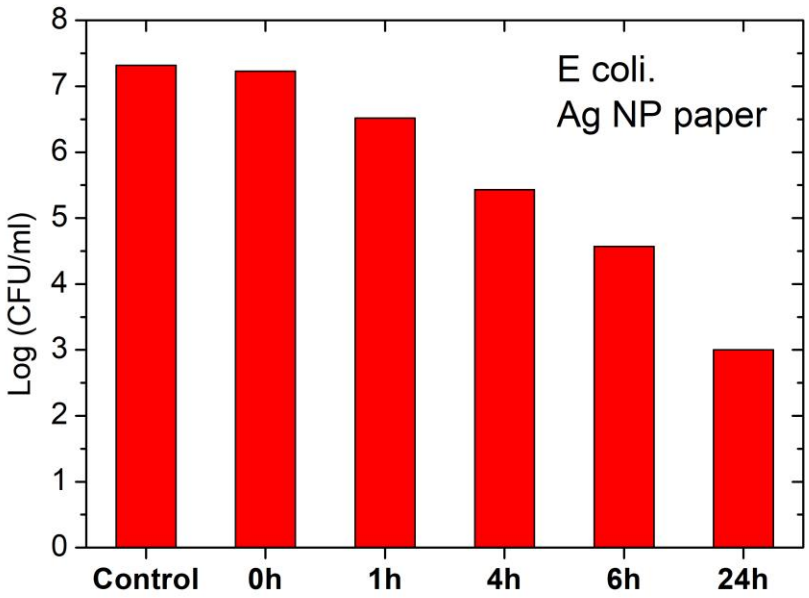

Figure 4. Antimicrobial test of AgNP impregnated paper on E-coli and leaching from the paper substrate. Please note the logarithmic scale on the y-axis.

In order to investigate the leaching behavior of the AgNPs, the substrates were prepared with two different loadings of silver via addition of 1 and 2 ml of the colloidal NP solution to the fines dispersion. The filtrate after formation of the sheets was colorless indicating that the AgNPs had been quantitatively incorporated into the sheets. Considering the total amount of Ag in the dispersion this correlates to an Ag content of 10 and 20 µg, respectively, in the sheets, which equals to 42 and 84 µg Ag per gram of paper. The relative mass of leaching AgNPs as well as total leached mass of AgNPs after exposure to water under rigorous shaking is depicted in Figure 5.

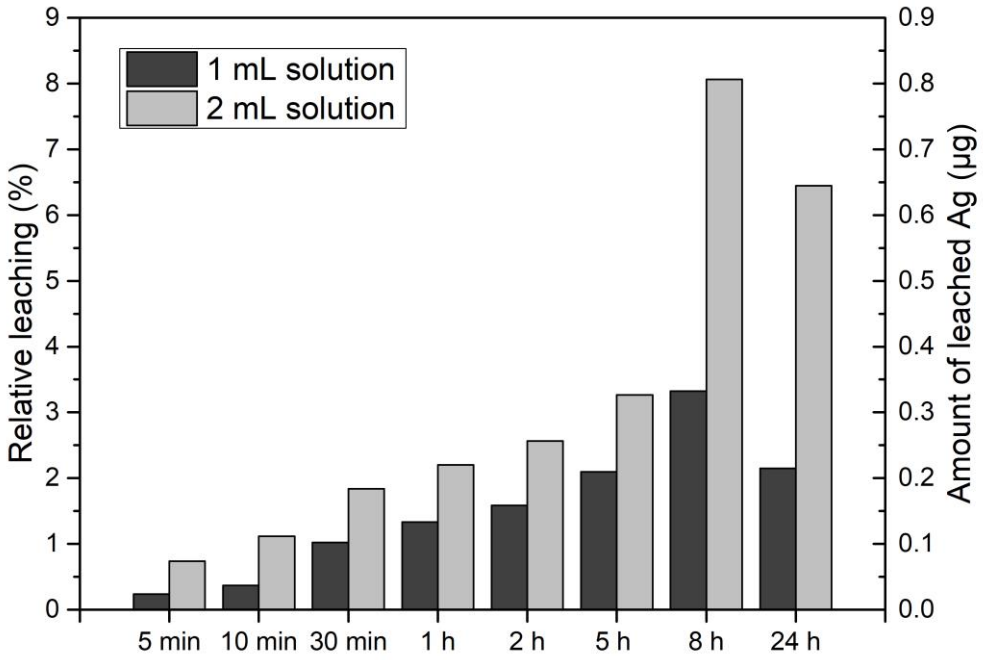

Figure 5. Figure 5. Relative amount of leached Ag in comparison to the Ag used for the sheet formation. For the tests, 1 and 2 ml of the colloidal Ag dispersion (10 µg/ml Ag) were added to the fines suspension.

4. Discussion

The use of LAL for the generation of AgNPs which were then implemented into a microstructured paper substrate is a step towards a scalable approach to implement these nanoparticles into cellulosic materials. There are several advantages of this approach: the amount of applied nanoparticles can be precisely controlled, which is hardly possible with any of the other methods. This is important to avoid overdosing and to equip materials with just the required amount of nanoparticles to prevent bacterial growth, which is beneficial from both ecologic and economic point of view. Nearly any type of bulk material can be used to generate the nanoparticles by LAL, and the use of reduction and capping agents can be avoided. In the case of the AgNPs, there is a thin oxide layer resulting in negatively charged surface (ζ = -50 mV) making them stable in colloidal solution according to the DLVO theory [44]. On the other hand, paper fines represent an underutilized stream in paper industry and technology, which have a few positive and several negative properties in the course of the paper manufacturing process. One of their drawbacks in paper production, namely their tendency to strongly interact with colloids, is exploited in the case of nanoparticles. After mixing the AgNPs with paper fines suspensions, the colored NPs are homogeneously distributed in the fines' suspensions. Any precipitation of the AgNP is not observed while aggregates on the fines surface are very rare. There must be some sort of interaction of these AgNPs with the fines, since during the sheet formation process, any removal of the AgNPs has not been observed, since the filtrates did not exhibit any color. In contrast, the sheets are slightly yellowish.

The concentrations of silver in our system are rather small with just 10 AgNPs per µm², still these AgNP decorated sheets exhibit antimicrobial activity which was our main goal. There are two types of particles, those that are directly in contact with the bacteria during testing and those which are buried inside the paper network, thereby slowly providing silver ions over time. The action mechanism of silver nanoparticles on bacteria is still not completely clear and fully understood, but

the concentration, shape and size of AgNPs are known to have a significant effect on the inactivation effectiveness [45, 46]. After the penetration of AgNPs inside the bacteria, NPs interact with intracellular materials, DNA loses its replication ability and cellular proteins are inactivated [47].

Recent investigations into the antimicrobial activity indicated that bacterial growth is not suppressed by affecting the maximum growth rate but by extension of the lag phase, i.e. the time bacteria spend without replicating and adapting to a new environment. A continuous release of Ag^+ ions exhibits higher antimicrobial effects than adding a specific amount of Ag^+ at the beginning of the experiment [48]. Further, electrically generated Ag^+ has better antimicrobial properties than other silver-based compounds [49-51].

Upon immersion in water under vigorous shaking, a small fraction of the AgNPs was leaching from the paper. The determined concentration increased slowly for a period of 8 h, whereas leaching directly correlated with the amount of particles in the paper. After 8 h of exposure to water, the paper network disassembled, leading to a burst of released silver in the solution. One might expect that these levels are going to rise for the 24 h sample but the silver levels in the solution, are smaller than after 8 hours. Most likely, the AgNP are readsorbing and reattaching into fines which were abraded from the paper substrates during the shaking process.

5. Conclusions

We proposed a simple, fast and environmentally friendly method to fabricate AgNP impregnated paper fines sheets with antimicrobial activity. The method is based on standard route for paper sheet formation where a step of addition of colloidal nanoparticles is added. The method works for any types of colloidal nanoparticle solutions synthesized by LAL while high stability of nanoparticle solution (high ζ potential) is required for better dispersion into paper solution and thus better homogeneity in the final product.

Further improvement of antimicrobial activity will be assessed by optimizing the nanoparticle number density and by using different types of LAL nanoparticles (Cu, Ti). Future development of the method will be realized in terms of applications of broad range of nanoparticles with unique properties (Cu, Ti, metal-oxides, two-component) for different applications (catalysis, photoactivity, sensors).

Supplementary Materials:

Acknowledgments: This work has been partially supported by project IP-11-2013-2753 funded by the Croatian Science Foundation and by Austrian Academy of Science under Joint Excellence in Science and Humanities fund. NK acknowledge the COST Action TD 1208 for fruitful discussions. *E. coli* K12 was donated by Laboratory for Biology and Microbial Genetics, Faculty of Food Technology and Biotechnology, University of Zagreb (Zagreb, Croatia).

Author Contributions: W.S. analyzed data and partially wrote the article. W.F., D.B., W.B. and N.K. performed experiments with sheet formation and AgNP impregnation. A.Z., G.F. and A.J. performed SEM and EDX measurements and analysis. S.S. and N.K. wrote the main body paper and analyzed data. D.B. and N.K. synthesized and analyzed AgNPs. T.V. performed antimicrobial tests. W.G. performed leaching tests.

Conflicts of Interest: The authors declare no conflict of interest. The founding sponsors had no role in the design of the study; in the collection, analyses, or interpretation of data; in the writing of the manuscript, and in the decision to publish the results.

References

1. Reishofer, D.; Rath, T.; Ehmann, H.M.; Gspan, C.; Dunst, S.; Amenitsch, H.; Plank, H.; Alonso, B.; Belamie, E.; Trimmel, G.; Spirk, S. *ACS Sustain. Chem. Eng.* **2017**, *5*, 3115–3122, 10.1021/acssuschemeng.6b02871.
2. Breitwieser, D.; Kriechbaum, M.; Ehmann, H.M.A.; Monkowius, U.; Coseri, S.; Sacarescu, L.; Spirk, S. Carbohydr. Polym. 2015, 116, 261-266.
3. Breitwieser, D.; Spirk, S.; Fasl, H.; Ehmann, H.M.A.; Chemelli, A.; Reichel, V.E.; Gspan, C.; Stana-Kleinschek, K.; Ribitsch, V. *J. Mat. Chem. B* **2013**, *1*, 2022-2030.
4. Sahoo, K.; Biswas, A.; Nayak, J. *Sens. Actuators, A* **2017**, *267*, 99-105.
5. Spiridonov, V.V.; Panova, I.G.; Makarova, L.A.; Afanasov, M.I.; Zezin, S.B.; Sybachin, A.V.; Yaroslavov, A.A. *Carbohydr. Polym.* **2017**, *177*, 269-274.
6. Van Rie, J.; Thielemans, W.; *Nanoscale* **2017**, *9*, 8525-8554.
7. Croes, S.; Stobberingh, E.E.; Stevens, K.N.J.; Knetsch, M.L.W.; Koole, L.H. *ACS Appl. Mater. Interfaces* **2011**, *3*, 2543-2550.
8. Shrivastava, S.; Bera, T.; Singh, S.K.; Singh, G.; Ramachandrarao, P.; Dash, D. *ACS Nano* **2009**, *3*, 1357-1364.
9. Reishofer, D.; Ehmann, H.M.; Amenitsch, H.; Gspan, C.; Fischer, R.; Plank, H.; Trimmel, G.; Spirk, S. *Carbohydr. Polym.* **2017**, *164*, 294-300.
10. Schlücker, S. SERS Microscopy: nanoparticle Probes and Biomedical Applications. *Chem. Phys. Chem.* **2009**, *10*, 1344-1254, 10.1002/cphc.200900119.
11. Taajamaa, L.; Rojas, O.J.; Laine, J.; Yliniemi, K.; Kontturi, E. *Chem. Commun.* **2013**, *49*, 1318-1320.
12. Zhicong, M.; Zilin, G.; Ruoxia, C.; Xiaoqing, Y.; Zhiqiang, S.; Wei, G. *Current Medicinal Chemistry* **2018**, *25*, 1-25.
13. Coseri, S.; Spatareanu, A.; Sacarescu, L.; Rimbu, C.; Suteu, D.; Spirk, S. Harabagiu, V.; *Carbohydr. Polym.* **2015**, *116*, 9-17.
14. Donati, I.; Travan, A.; Pelillo, C.; Scarpa, T.; Coslovi, A.; Bonifacio, A.; Sergo, V.; Paoletti, S. *Biomacromolecules* **2009**, *10*, 210-213.
15. Dahl, J.A.; Maddux, B.L.S.; Hutchison, J.E. *Chem. Rev.* **2007**, *107*, 2228-2269.
16. Huang, H.; Yang, X. *Carbohydr. Res.* **2004**, *339*, 2627-2631.
17. Breitwieser, D.; Moghaddam, M. M.; Spirk, S.; Baghbanzadeh, M.; Pivec, T.; Fasl, H.; Ribitsch, V.; Kappe, C.O. *Carbohydr. Polym.* **2013**, *94*, 677-686.
18. Ehmann, H.M.A.; Breitwieser, D.; Winter, S.; Gspan, C.; Koraimann, G.; Maver, U.; Sega, M.; Köstler, S.; Stana-Kleinschek, K.; Spirk, S.; Ribitsch, V. *Carbohydr. Polym.* **2015**, *117*, 34-42.
19. Yan, G. Laser Ablation in Liquids: Principles and Applications in the Preparation of nanomaterials, Pan Stanford Publishing, Singapore, 2012, 9789814310956.
20. Barcikowski, S.; Mafuné, F. Trends and Current Topics in the Field of Laser Ablation and Nanoparticle Generation in Liquids. *J. Phys. Chem. C* **2011**, *115*, 4985–4985, 10.1021/jp111036a.
21. Zeng, H.; Du, X.-W.; Singh, S.C.; Kulinich, S.A.; Yang, S.; He, J.; Cai, W. Nanomaterials via laser ablation/irradiation in liquid: A review. *Adv. Funct. Mater.* **2012**, *22*, 1333–1353, 10.1002/adfm.201102295.
22. Zhang, D.; Gökce, B.; Barcikowski, S. Laser Synthesis and Processing of Colloids: Fundamentals and Applications. *Chem. Rev.* **2017,** *117*, 3990−4103, 10.1021/acs.chemrev.6b00468.
23. Besner, S.; Kabashin, A.V.; Winnik, F.M.; Meunier, M. Ultrafast laser based "green" synthesis of non-toxic nanoparticles in aqueous solutions. *Phys. A* **2008**, *93*, 955–959, 10.1007/s00339-008-4773-y.
24. Dolgaev, S.I.; Simakin, A.V.; Voronov, V.V.; Shafeev, G. A.; Bozon-Verduraz, F. nanoparticles produced by laser ablation of solids in liquid environment. *Appl. Surf. Sci.* **2002**, *186*, 546-551, 10.1016/S0169-4332(01)00634-1.
25. Tarasenko N.V.; Butsen, A.V. Laser synthesis and modification of composite nanoparticles in liquids. *Quantum Electron.* **2010**, *40*, 986-1003, 10.1070/QE2010v040n11ABEH014446.
26. Tsuji, T.; Watanabe, N.; Tsuji, M. Laser induced morphology change of silver colloids: formation of nano-size wires. Appl. Surf. Sci. **2003**, *211*, 189-193, 10.1016/S0169-4332(03)00225-3.
27. Tsuji, T.; Okazaki, Y.; Higuchi, T.; Tsuji, M. Laser-induced morphology changes of silver colloids prepared by laser ablation in water Enhancement of anisotropic shape conversions by chloride ions. *J. Photochem. Photobiol. A* **2006**, *183*, 297-303, 10.1016/j.jphotochem.2006.05.021.

28. Zeng, H.; Yang, S.; Cai, W. Reshaping Formation and Luminescence Evolution of ZnO Quantum Dots by Laser-Induced Fragmentation in Liquid. *J. Phys. Chem. C* **2011**, *115*, 5038-5043, 10.1021/jp109010c.
29. Giorgetti, E.; Giammanco, F.; Marsili, P.; Giusti, A. Effect of Picosecond Postirradiation on Colloidal Suspensions of Differently Capped AuNPs. *J. Phys. Chem. C* **2011**, 115, 5011-5020, 10.1021/jp108042m.
30. Burakov, V.S.; Tarasenko, N.V.; Butsen, A.V.; Rozantsev, V.A.; Nedel'ko, M.I. Formation of nanoparticles during double-pulse laser ablation of metals in liquids. *Eur. Phys. J. Appl. Phys.* **2005**, *30*, 107-112, 10.1051/epjap:2005016.
31. DeGiacomo, A.; DeBonis, A.; Dell'Aglio, M.; De Pascale, O.; Gaudiuso, R.; Orlando, S.; Santagata, A.; Senesi, G. S.; Taccogna, F.; Teghil, R. Laser Ablation of Graphite in Water in a Range of Pressure from 1 to 146 atm Using Single and Double Pulse Techniques for the Production of Carbon Nanostructures. *J. Phys. Chem. C* **2011**, *115*, 5123–5130, 10.1021/jp109389c.
32. Dell'Aglio, M.; Gaudiuso, R.; El Rashedy, R.; De Pascale, O.; Palazzo, G.; De Giacomo, A. Collinear double pulse laser ablation in water for the production of silver nanoparticles. *Phys. Chem. Chem. Phys.* **2013**, *15*, 20868-20875, 10.1039/C3CP54194K.
33. Krstulovic, N.; Shannon, S.; Stefanuik, R.; Fanara, C. Underwater-laser drilling of aluminum. *Int. J. Adv. Manuf. Technol.* **2013,** *69*, 1765-1773, 10.1007/s00170-013-5141-4.
34. Krstulovic, N.; Umek, P.; Salamon, K.; Capan, I. Synthesis of Al-doped ZnO nanoparticles by laser ablation of ZnO:Al_2O_3 target in water. *Mater. Res. Express* **2017**, *4*, 105003, 10.1088/2053-1591/aa896d.
35. Krstulovic, N.; Salamon, K.; Budimlija, O.; Kovac, J.; Dasovic, J.; Umek, P.; Capan, I. Parameters optimization for synthesis of Al-doped ZnO nanoparticles by laser ablation in water. *Appl. Surf. Sci.* **2018**, *15*, 916-925, 10.1016/j.apsusc.2018.01.295.
36. Krstulovic, N.; Milosevic, S. Drilling enhancement by nanosecond–nanosecond collinear dual-pulse laser ablation of titanium in vacuum. *Appl. Surf. Sci.* **2010**, *256*, 4142-4148, 10.1016/j.apsusc.2010.01.098.
37. Fischer, W.J.; Mayr, M.; Spirk, S.; Reishofer, D.; Jagiello, L.A.; Schmiedt, R.; Colson, J.; Zankel, A.; Bauer, W. Pulp Fines—Characterization, Sheet Formation, and Comparison to Microfibrillated Cellulose. *Polymers* **2017**, *9*, 366, 10.3390/polym9080366.
38. Kiss, L. B.; Söderlund, J.; Niklasson, G. A.; Granqvist, C. G. New approach to the origin of lognormal size distributions of nanoparticles. *Nanotechnology* **1999,** *10*, 25–28, 10.1088/0957-4484/10/1/006.
39. Söderlund, J.; Kiss, L. B.; Niklasson, G. A.; Granqvist, C. G. Lognormal size distributions in particle growth processes without coagulation. *Phys. Rev. Lett.* 1998, *80*, 2386-2388, 10.1103/PhysRevLett.80.2386.
40. Mafuné, F.; Kohno, J.; Takeda, Y.; Kondow, T. Formation and Size Control of Silver Nanoparticles by Laser Ablation in Aqueous Solution. *J. Phys. Chem. B* **2000**, *104*, 9111-9117, 10.1021/jp001336y.
41. Zeng, H.; Du, X.-W.; Singh, S. C.; Kulinich, S. A.; Yang, S.; He, J.; Cai, W. Nanomaterials via Laser Ablation/Irradiation in Liquid: A Review. *Adv. Funct. Mater.* **2012**, *22*, 1333-1353, 10.1002/adfm.201102295.
42. Zhang, D.S.; Liu, J.; Liang, C.H. Perspective on how laser-ablated particles grow in liquids. Sci. China-Phys. Mech. Astron. 60 (2017) 074201.
43. Lyklema, J.; van Leeuwen, H. P. Minor, M.; *Adv. Colloid Interface Sci.* **1999**, *83*, 33-69.
44. Agnihotri, S.; Mukherji, S.; Mukherji, S. Size-controlled silver nanoparticles synthesized over the range 5–100 nm using the same protocol and their antibacterial efficacy. *RSC Adv.* **2014**, *4*, 3974-3983, 10.1039/C3RA44507K.
45. Sondi, I.; Salopek-Sondi, B. Silver nanoparticles as antimicrobial agent: a case study on E. coli as a model for Gram-negative bacteria. *J. Colloid Interface Sci*. **2004**, *275*, 177-182, 10.1016/j.jcis.2004.02.012.
46. Morones, J. R.; Elechiguerra, J. L.; Camacho, A.; Holt, K.; Kouri, J. B.; Ramírez, J. T.; Yacaman, M. J. The bactericidal effect of silver nanoparticles. *Nanotechnology*, **2005**, *16*, 2346-2353, 10.1088/0957-4484/16/10/059.
47. Liau, S.; Read, D.; Pugh, W.; Furr, J.; Russell, A. Interaction of silver nitrate with readily identifiable groups: relationship to the antibacterialaction of silver ions. *Lett. Appl. Microbiol*. **1997**, *25*, 279-283, 10.1046/j.1472-765X.1997.00219.x.
48. Berger, T.; Spadaro, J.; Bierman, R.; Chapin, S.; Becker, R. Antifungal properties of electrically generated metallic ions. *Antimicrob. Agents Chemother*. **1976**, *10*, 856-860, 10.1128/AAC.10.5.856.
49. Berger, T.; Spadaro, J.; Chapin, S.; Becker, R. Electrically generated silver ions: quantitative effects on bacterial and mammalian cells. *Antimicrob. Agents Chemother*. **1976**, *9*, 357-358, 10.1128/AAC.9.2.357.
50. Vukusic, T.; Shi, M.; Herceg, Z.; Rogers, S.; Estifaee, P.; Mededovic Thagard, S. Liquid-phase electrical discharge plasmas with a silver electrode for inactivation of a pure culture of Escherichia coli in water. *Innov. Food Sci. Emerg. Technol.* **2016**, *38*, 407-413, 10.1016/j.ifset.2016.07.007.